Structure and Speciation in Hydrous Silica Melts. 2. Pressure Effects

Kelly E. Anderson,[†] Lorna C. Grauvilardell,[†] Marc M. Hirschmann,[‡] and J. Ilja Siepmann*,[†]

Departments of Chemistry and of Chemical Engineering and Materials Science, University of Minnesota, 207 Pleasant Street SE, Minneapolis, Minnesota 55455-0431, and Department of Geology and Geophysics, University of Minnesota, 310 Pillsbury Drive SE, Minneapolis, Minnesota 55455-0219

Received: March 14, 2008; Revised Manuscript Received: July 22, 2008

The effect of pressure on structure and water speciation in hydrated liquid silica is examined over a range of temperatures and compositions. The Feuston−Garofalini (FG) potential is used in isobaric−isothermal Monte Carlo simulations carried out at four pressures (0.25, 1.0, 2.5, and 10 GPa) for seven temperatures ($2000 \leq T \leq 9000$ K) and five compositions ($0.0 \leq x_w \leq 0.4$). The FG potential yields a stable melt phase for $p \geq 1.0$ GPa and/or $x_w \leq 0.1$ for all temperatures. The volume minimum seen in previous simulations of pure and hydrated liquid silica using the FG potential persists up to 2.5 GPa but is no longer evident at 10 GPa. This is correlated with gradual structural changes of the liquid up to 2.5 GPa and with more significant changes at 10 GPa. Even at high overall concentrations of water ($x_w = 0.4$), only about 2% of oxygen atoms are present as molecular water species at the lowest temperature. This percentage decreases with increasing pressure and temperature.

1. Introduction

Understanding pressure-induced changes in structure, dynamics, and speciation of pure and hydrous silica (SiO_2) liquids is of great interest for gaining insight into geologically relevant melts (magmas). Previous experimental[1−3] and theoretical[4−10] studies have focused primarily on amorphous and liquid silica at pressures from 1 bar to 150 GPa. It has been shown that upon increasing pressure, the Si−O coordination number shifts from four at lower pressures toward six at pressures above 20 GPa, leading to a significant densification of the system.[1−3]

Few theoretical studies have examined the effect of pressure on hydrated liquid silica, although a variety of experimental studies are available on solubility and melting relations between SiO_2 and H_2O.[11] The solubility of H_2O in liquid silica increases as temperature and pressure increase, particularly as the critical point in the binary quartz-melt-fluid equilibrium (1100 °C, 0.97 GPa) is approached.[12,13] These experimental studies have primarily focused on $p < 2$ GPa and $T < 2000$ K. Challenges exist in making accurate measurements at the concurrent pressures and temperatures of geophysical relevance.[14] Simulation provides an ideal alternative for gaining insight into the microscopic properties of the SiO_2-H_2O system.

In this paper, we focus on the pressure range $0.25 \text{ GPa} \leq p \leq 10$ GPa and study the effect of pressure on structure and water speciation in silica-rich liquids using Monte Carlo simulation. The companion to this paper[15] provides a detailed investigation to the temperature and composition effects at 1.0 GPa.

2. Simulation Details

Monte Carlo (MC) simulations were performed in the isobaric−isothermal ensemble[16] using the atom-based Feuston−Garofalini (FG) potential for silica and water.[17,18] The FG potential allows Si−O and H−O bonds to break and form as well as starting units (SiO_2 and H_2O molecules) to evolve into new species (e.g., Si−O−Si triads in a tetrahedral network or SiOH units). Details of our implementation of the FG potential can be found in ref 15. Phase space was sampled using atomic translation moves and volume changes, and periodic boundaries were used to mimic a bulk system.

Simulations were performed over a temperature range from 2000−9000 K. Each system was initially heated to 9000 K and allowed to equilibrate. The final configuration was used as the initial configuration for the next lowest temperature. Steps of 1500 K were used between 9000 and 3000 K and of 500 K between 3000 and 2000 K. At each temperature, the system was initially equilibrated for 2×10^5 MC cycles (where each cycle consists of N steps) and ensemble averages were collected over 3×10^6 MC cycles. This procedure was followed at pressures of 0.25, 2.5, and 10 GPa. Data at 1.0 GPa are from ref 15 where a slightly different cooling protocol was followed. A system size consisting of 60 formula units (180 atoms) was used at $p = 0.25$ GPa while 80 formula units (240 atoms) were used for 2.5 and 10 GPa. Five compositions were studied: pure silica, referred to as 0W, and overall mole fractions of water, x_w, equal to 0.1, 0.2, 0.3, and 0.4, referred to as 10W, 20W, 30W, and 40W, respectively. For each composition, the overall number of atoms was held constant and the ratio of SiO_2:H_2O formula units was varied to reach the appropriate overall mole fraction of water.

Five independent simulations were performed at each state point, starting from different initial densities and configurations. All properties are averaged over these five simulations. Error bars indicate the standard error of the mean over these simulations.

3. Results and Discussion

3.1. Stability of the Melt. Since this simulation study covers extremely high temperatures at relatively modest pressures and relatively high water content (compared to the Earth's mantle), one first needs to establish whether stable hydrous silica melt

* Corresponding author. E-mail: siepmann@umn.edu.
† Departments of Chemistry and of Chemical Engineering and Materials Science.
‡ Department of Geology and Geophysics.

10.1021/jp802255y CCC: $40.75
Published on Web 09/24/2008

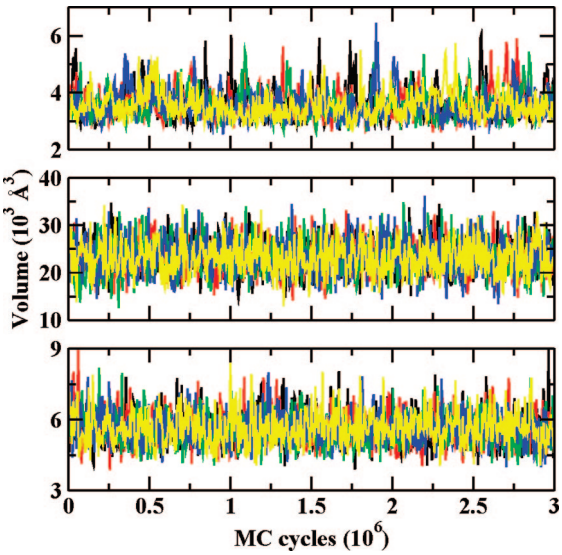

Figure 1. Evolution of the system volume during the production period of three simulations at $T = 9000$ K for $x_w = 0.0/p = 0.25$ GPa (top), $x_w = 0.4/p = 0.25$ GPa (middle), and $x_w = 0.4/p = 1.0$ GPa (bottom). The different colors show data for the five independent simulations.

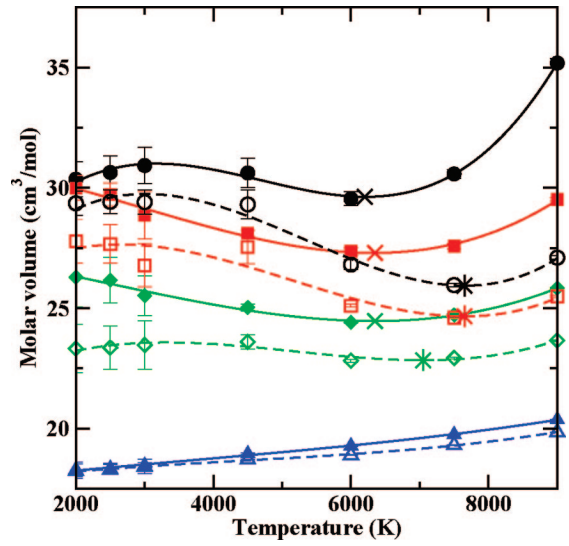

Figure 2. Molar volume versus temperature for $x_w = 0.0$ (open symbols/dashed lines) and 0.1 (closed symbols/solid lines) at various pressures. Circles, squares, diamonds, and upright triangles denote $p = 0.25$, 1.0, 2.5, and 10 GPa, respectively. The lines show a third-order polynomial fit to the data. For those fits with a minimum falling into the temperature interval investigated here, the cross or star indicates the position of the volume minimum. Error bars indicated the standard error of the mean.

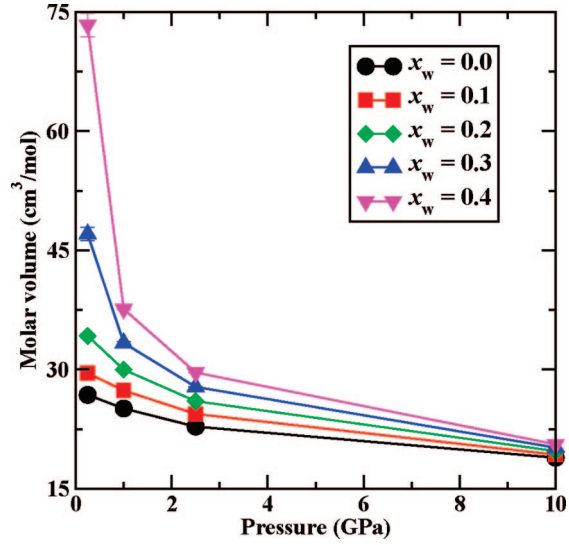

Figure 3. Molar volume versus pressure at $T = 3000$ K. The lines are drawn as a guide for the eye. Error bars indicate the standard error of the mean.

phases are present for the FG force field at all state points. Figure 1 shows the evolution of the system volume for three systems at 9000 K, and it is clear that all systems show fluctuations of the system volume around a mean value without a drift over the production period. However, the average volume for the 40W system at 0.25 GPa is much larger than those of the other two trajectories shown. Structural analysis demonstrates that this system is indeed a low-density phase with isolated aggregates and not a continuous silica network. A good indicator of such low-density aggregate structures is the $g(r)$ value at the first minimum in the Si−Si or O−O radial distribution functions (RDFs). For a melt, one can expect that this value falls significantly below unity, while the aggregate form can exhibit values above unity and a decrease of the $g(r)$ value from the first to the second minimum. For simplicity, we define that the aggregate form is stable for cases where both the $g(r)$ values at the first minimum of the Si−Si and O−O RDFs are greater than unity. Using this criterion, all simulations at $p \geq 1.0$ GPa and/or with $x_w \leq 0.1$ yield stable melts, but the following simulations ($p = 0.25$ GPa) yield the aggregate form and are not further analyzed in the remainder of this work: system 20W at $T = 9000$ K, system 30W at $T \geq 7500$ K, and system 40W at $T \geq 6000$ K. That is, high pressure and low water content stabilize the melt phase.

3.2. Molar Volume. Figure 2 shows isobars of the molar volume (V_m) per formula unit calculated for the FG potential as a function of temperature for neat liquid silica and hydrated liquid silica with $x_w = 0.1$. For the neat silica system, V_m at 2000 K and 1.0 GPa is 27.8 ± 0.9 cm^3/mol, which is in good agreement with the experimental data.[19] As the pressure changes, V_m increases to 29.4 ± 0.5 cm^3/mol at 0.25 GPa and decreases to 23.3 ± 1.0 cm^3/mol at 2.5 GPa. These values are slightly higher (by 1−2 cm^3/mol) than those given by the fit to experimental data,[19] but this is primarily due to the temperature difference (1673 versus 2000 K here). In the region $3000 < T < 9000$ K, pure FG silica exhibits a volume depression.[15,20] This depression region persists up to 2.5 GPa, with the temperature of the volume minimum shifting to lower values with pressure. At 10 GPa, this depression is no longer present and V_m increases steadily by 9% from 2000 to 9000 K.

With the addition of 10 mol % water ($x_w = 0.1$), the volume depression remains but is shifted to lower temperatures compared to neat silica. For system 10W, the volume minimum slightly increases from 6200 to 6350 K when the pressure is increased from 0.25 to 1.0 GPa. As for neat silica, system 10W at 10 GPa no longer shows any volume depression in the region from 2000 to 9000 K and V_m increases monotonically by 11%. At 10 GPa, the molar volumes for systems 0W and 10W are very close over the entire pressure range. At lower pressures, though, the FG simulations yield smaller V_m for pure silica, by as much as 23% at 0.25 GPa and 9000 K relative to $x_w = 0.1$.

The effect of hydration on the molar volume of silica changes greatly with pressure (see Figure 3). At high pressure (10 GPa), the molar volume of the hydrated liquid silica system with $x_w = 0.4$ is only 8% larger than that of the pure silica system at 3000 K. At 0.25 GPa and 3000 K, the molar volume for system

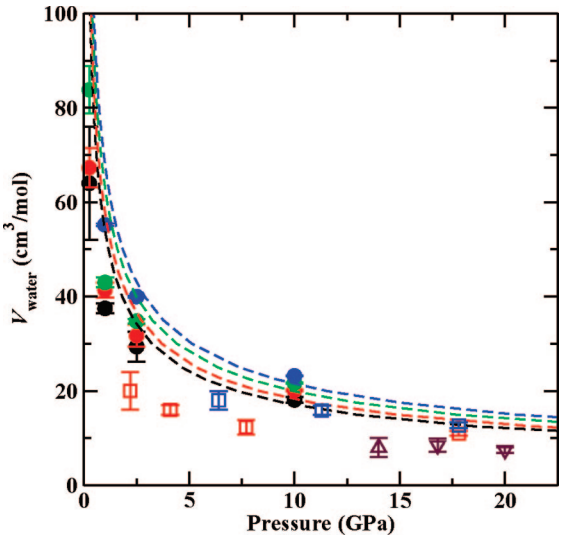

Figure 4. Partial molar volume of water as a function of pressure. Filled circles denote composition-independent fits to the simulation data for the FG potential; squares show data from first principles molecular dynamics (FPMD) simulations of hydrous $MgSiO_3$ melts;[24] the triangles indicate data from high-pressure experiments for silicates at $T = 2170$ K by Matsukage et al.[22] (upright triangles) and at 2470 K by Sakamaki et al.[23] (downward triangles). The dashed line denotes the molar volume for pure water as given by the Pitzer−Sterner equation of state (EOS).[21] Black, red, green, and blue colors represent the simulation data and EOS at 2000, 3000, 4500, and 6000 K, respectively. Errors bars for the FG data indicate an 80% confidence interval over the results from five simulations.

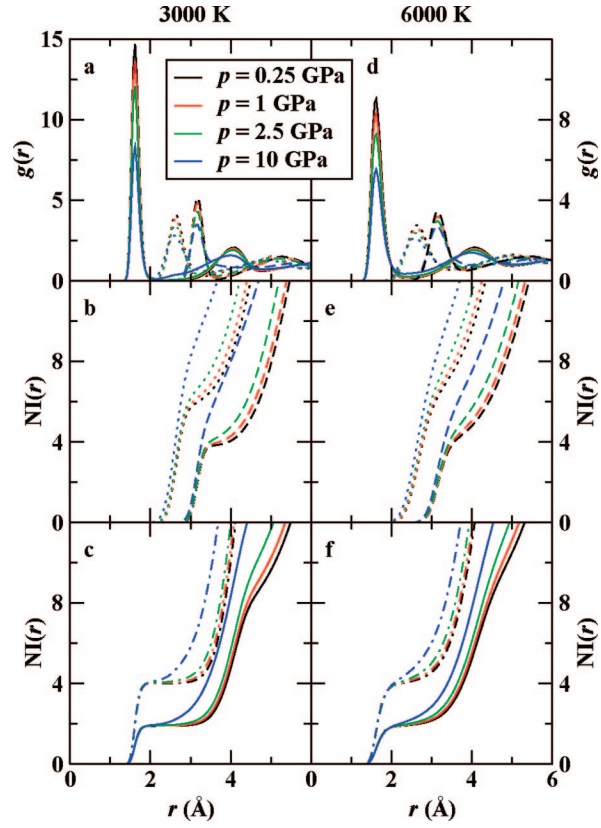

Figure 5. Radial distribution functions and number integrals for hydrated silica with $x_w = 0.1$ at $T = 3000$ K (left column) and at 6000 K (right column). Solid, dashed, and dotted lines indicate Si−O, Si−Si, and O−O RDFs. For the NIs, the same convention is used but with solid and dash-dotted lines indicating O−Si and Si−O, respectively.

40W is nearly three times larger than for system 0W. That is, pressure effects on the molar volume are much more pronounced for highly hydrated silica. Although a continuous silica network persists for system 40W at 3000 K, this system and other systems with $V_m > 35$ cm^3/mol also contain low density bubbles filled with molecular fragments.

The partial molar volume of water, V_{water}, obtained from composition-independent fits (see ref 15) to the simulation data for the FG model is depicted in Figure 4. The general shape of the pressure dependence of V_{water} for the silica melt closely resembles that found for the molar volume of pure water, $V°$.[21] At $p \leq 2.5$ GPa, V_{water} in the silica melt is smaller than $V°$, but the differences diminish with increasing temperature and pressure, i.e. dissolution in the silica network and conversion of water to silanols (see below) leads to a negative volume of mixing. At $p = 10$ GPa, V_{water} for the FG silica melt is slightly larger than $V°$. This indicates that the repulsive part of the FG potential is somewhat too steep. Experimental measurements[22,23] and first principles simulations[24] for hydrous silicate melts also yield $V_{water} < V°$, but the differences are larger than those found here for the silica melt, i.e. the presence of ions, such as Mg^{2+}, leads to a further reduction in V_{water}.

3.3. Liquid Structure. ***A. Radial Distribution Functions.*** Figure 5 shows the Si−Si, O−O, and Si−O radial distribution functions (RDFs) and number integrals (NIs) for each pressure at 3000 and 6000 K for the system with $x_w = 0.1$. (The histogram bin width is 0.04 Å for all RDFs.) The corresponding locations for the first peak and first minimum and the coordination numbers are listed in Table 1. At 3000 K, between 0.25 and 2.5 GPa, the structure of the hydrated liquid does not change substantially. A slight decrease in the height of the first peak is seen for each atom pair but the location and shape of these peaks remain constant over this pressure interval.

In contrast, raising the pressure to 10 GPa leads to more noticeable changes in structure. Although the position of the first peak of the Si−O RDF does not change, its second peak broadens significantly toward shorter separation distances, with a slight shoulder forming at 2.75 Å. The first peak of the O−O RDF broadens in both directions and the peak position shifts slightly to a shorter distance. For Si−Si, the shape and position of the first peak is similar to that of the lower pressure RDFs but the first minimum is less pronounced and the second peak disappears. At 6000 K, the RDFs at 10 GPa are more similar to those at the three lower pressures. While some slight broadening is seen in the Si−Si and O−O RDFs as pressure increases, there are no stark structural changes as a function of pressure.

Analysis of the NI, or the average coordination number (CN) at the first minimum of the RDF, r_M, for a given atom pair (Figure 5 and Table 1), confirms the similarity among all pressures for the Si−O pairs. For Si−O and O−Si, the average coordination in the first shell is close to four and two, respectively, at both 3000 and 6000 K regardless of pressure in this region. As the pressure increases, the CNs shift to slightly higher values (by 3% at 3000 K and by 7% at 6000 K). This is consistent with experimental findings that the increase in CN is minimal for $p < 20$ GPa.[1−3] However, some previous theoretical studies for amorphous and liquid silica[8,10,25,26] indicated that the coordination of O around Si shifts from 4-fold toward 6-fold with increasing pressure.

Examining the second nearest neighbor sphere, differences for Si−Si and O−O pairs arise as pressure changes. For Si−Si, the CN at $T = 3000$ K and $p = 0.25$ GPa is 3.85, slightly below the ideal tetrahedral CN. As the pressure increases, the CN increases 3% to 3.98 at 1.0 GPa and then another 5% to 4.18 at

TABLE 1: First Peak and First Minimum Distances and Coordination Number at the First Minimum Calculated from the RDF and NI of Hydrated Silica ($x_w = 0.1$) at 3000 and 6000 K[a]

		Si−Si			O−O			Si−O			
T (K)	p (GPa)	r_P	r_M	CN	r_P	r_M	CN	r_P	r_M	CN_{SiO}	CN_{OSi}
3000	0.25	3.18	3.66	3.85	2.62	3.22	6.04	1.62	2.26	4.01	1.90
	1.0	3.18	3.70	3.98	2.62	3.26	6.34	1.62	2.22	4.02	1.90
	2.5	3.14	3.62	4.18	2.62	3.22	6.75	1.62	2.18	4.05	1.92
	10.0	3.14	3.78	6.90	2.58	3.50	11.0	1.62	2.14	4.13	1.96
6000	0.25	3.14	3.82	4.46	2.62	3.50	7.40	1.62	2.42	4.08	1.93
	1.0	3.14	3.90	4.83	2.62	3.50	7.76	1.62	2.42	4.12	1.95
	2.5	3.14	3.86	5.27	2.62	3.54	8.73	1.62	2.38	4.19	1.98
	10.0	3.14	3.98	7.41	2.58	3.54	10.9	1.62	2.30	4.36	2.07

[a] For Si−O, both SiO and OSi coordination numbers are provided.

2.5 GPa. At 10 GPa, the CN increases dramatically to 6.90. At 6000 K, the Si−Si CNs are always larger than at 3000 K (on average by 17%) and, again, increase by ≈70% from 0.25 to 10 GPa. The Si−Si CN of 7.41 at 6000 K and 10 GPa obtained for the FG potential is somewhat higher than the value of 6.7 computed by Karki et al.[10] from first principles molecular dynamics (FPMD) simulations at 6000 K.

The distributions of O−O pairs follow similar trends. At 3000 K, the O−O CN increases moderately from 6.04 at 0.25 GPa to 6.75 at 2.5 GPa, before reaching 11.0 at 10 GPa. Similarly at 6000 K, the O−O CN increases from 7.40 at 0.25 GPa to 10.9 at 10 GPa.

These trends in the Si−Si and O−O CNs can explain the lack of a volume depression at 10 GPa. From a previous simulation study,[27] Perchak and O'Reilly suggested that the volume depression is accompanied by a rise in CN. At 10 GPa, the CN of O−O is already significantly above the value of 6 expected for an ideal tetrahedral network; in fact, it is approaching 12, the close packing CN, as was also observed in FPMD simulations.[10] Further increases in CN beyond 12 appear unlikely, and the hydrated silica system at 10 GPa behaves like a regular fluid and does not show a volume minimum.

Of less importance, but still interesting to note, is that the Si−Si and O−O CNs show a larger increase upon a temperature increase from 3000 to 6000 K at a pressure of 2.5 GPa than at the lower pressures. Clearly, both temperature and pressure destabilize a tetrahedral liquid. Thus, the same temperature jump has a larger effect at higher pressures as long as these pressures alone are not sufficient to cause a rearrangement from an open tetrahedral structure to a close-packed liquid.

Figure 6 shows the temperature dependence of the O−O RDF at the lowest and highest pressure for the system with $x_w = 0.1$. At 0.25 GPa, the position of the first peak remains constant but the peak height decreases with increasing temperature and the peak broadens. There is a substantial shift of the first minimum to larger separation distances and shallower depths. This is repeated in the structure of the second peak. This peak, too, broadens with increasing temperature but remains centered at the same distance throughout. At 10 GPa, the temperature dependence of the first peak in the RDF is similar to the lower pressure, but changes arise beyond this. The first minimum is significantly less sharp as is the second peak. Additionally, the position of the second peak shifts to larger values of r with temperature. For each pressure, the average CN shifts relatively gradually with increasing temperature, but at 0.25 GPa the structure remains predominately tetrahedral (CN ≈ 6) over the entire temperature range, whereas it resembles a close-packed liquid over the entire temperature range at 10 GPa. We surmise that there exists an intermediate pressure (2.5 GPa < p < 10 GPa) where a change in temperature from 2000 to 9000 K would result in a collapse of the tetrahedral network.

B. Angular Distribution Functions. Significant structural changes of the tetrahedral network are also reflected in the

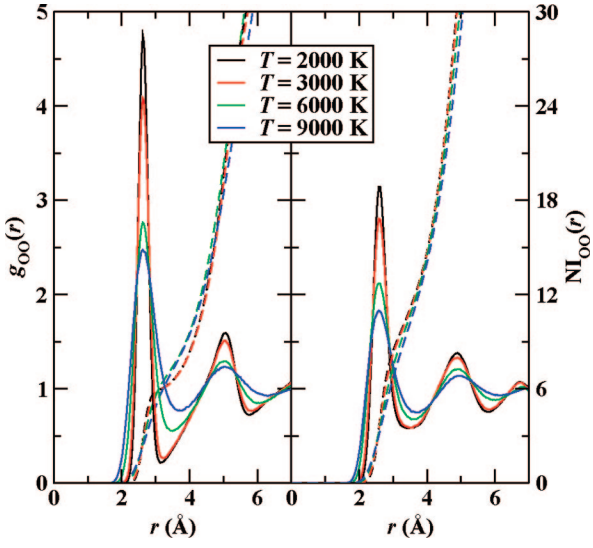

Figure 6. Temperature dependence of the O−O radial distribution function and number integral for $x_w = 0.1$ at 0.25 (left) and 10 GPa (right).

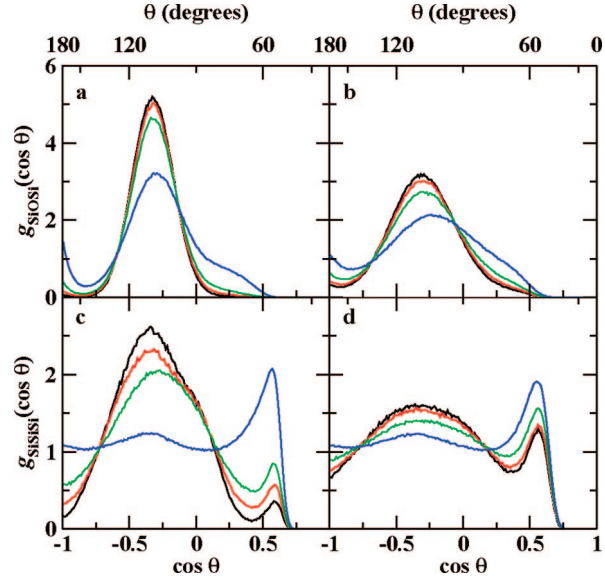

Figure 7. Angular distribution functions of the Si−O−Si bond (top) and Si−Si−Si neighbor (bottom) angles for $x_w = 0.1$. (a and c) 3000 K. (b and d) 6000 K. Colors as in Figure 5.

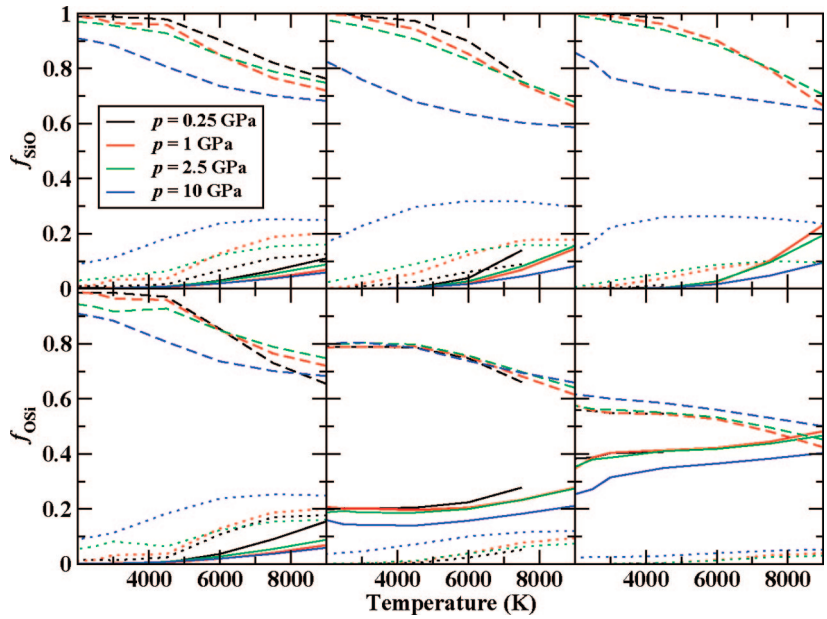

Figure 8. SiO_n (top) and OSi_n (bottom) coordination environments as a function of temperature for the pure silica system (left), $x_w = 0.2$ (center), and $x_w = 0.4$ (right). Dashed, solid, and dotted lines represent tetrahedral coordination (SiO_4/OSi_2), undercoordination (SiO_3/OSi_1), and overcoordination (SiO_5/OSi_3), respectively.

angular distributions at 3000 and 6000 K (see Figure 7). The FG potential uses three-body terms applied to Si−O−Si and O−Si−O angles to impose tetrahedral order on silica.[17,18] First, examining the Si−O−Si angle distribution at both temperatures, the height of the peak at the tetrahedral angle decreases with increasing pressure, but this decrease is relatively gradual from 0.25 to 2.5 GPa followed by more dramatic decrease in the peak height at 10 GPa. Furthermore, at the highest pressure, a second peak emerges for $\theta = 180°$ and the main peak shows a shoulder at $\theta \approx 75°$. This shift of the main peak toward smaller Si−O−Si angles with increasing pressure follows experimental trends[28] and agrees with FPMD simulations.[10] Relative to the system at $T = 3000$ K and $p = 1$ GPa, an increase of the pressure to 10 GPa has a more significant effect on distorting the tetrahedral network than an increase of the temperature to 6000 K.

Analyzing slightly longer-ranged interactions, the nonbond-bending angle Si−Si−Si of three neighboring Si atoms is not subject to any penalty function in the FG force field. At 3000 K, we again observe a gradual change in the distribution upon increasing the pressure from 0.25 to 2.5 GPa followed by a large change in the angular distribution at 10 GPa. At the lower pressures, the tetrahedral peak shifts to slightly smaller angles with increasing pressure, but more importantly, the minor peak for very small angles ($40° < \theta < 70°$) triples in intensity. At 10 GPa, only a small remnant of the tetrahedral peak remains and the peak near $\cos\theta = 0.5$ is dominant. The pressure dependence at 6000 K shows similar behavior, but the Si−Si−Si distribution is already quite broad even at low pressures. With the densification of the melt as pressure increases, the respective $Si-Si_4$ tetrahedra are compressed into closer proximity, and the peak at $\theta = 60°$ suggests that different tetrahedra interpenetrate, leading to very small Si−Si−Si angles.

C. Coordination Environments. The fraction of Si and O atoms with a given coordination number as a function of temperature at each pressure for systems 0W, 20W, and 40W is shown in Figure 8. A neighbor is defined as an atom within 2.35 Å of the atom of interest.[15] First, examining the coordination of Si at the lower three pressures, more than 95% of Si atoms have four O neighbors at $T \leq 4500$ K for all three

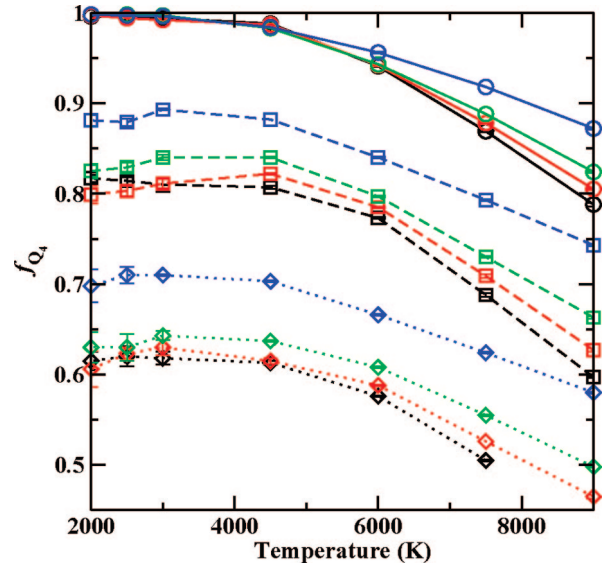

Figure 9. Fraction of Q_4 species as a function of temperature. Systems 0W, 10W, and 20W are depicted as circles/solid, squares/dashed, and diamonds/dotted lines, respectively. Black, red, green, and blue denote $p = 0.25$, 1.0, 2.5, and 10 GPa, respectively. Error bars show the standard error of the mean.

compositions, and f_{SiO_4} decreases to ≈70% for the stable melts at 9000 K. The fraction of overcoordinated Si atoms, f_{SiO_5}, increases for $T \leq 4500$ K but then reaches a plateau. In contrast, the fraction of undercoordinated Si atoms, f_{SiO_3}, remains near zero for $T \leq 4500$ K, and then increases for the higher temperatures.

The pressure increase to 10 GPa has a significant effect on the Si coordination, i.e. f_{SiO_5} is dramatically increased in particular at lower temperatures and correspondingly f_{SiO_4} is reduced to <90% for all compositions. However, f_{SiO_3} is significantly reduced at higher temperature, leading to a closing of the gap in f_{SiO_4} between the different pressures at 9000 K. The fraction of overcoordinated Si atoms found for the FG potential is slightly less than observed in FPMD simulations, where $f_{SiO_5} = 30\%$ near 3000 K and 10 GPa.[6,10]

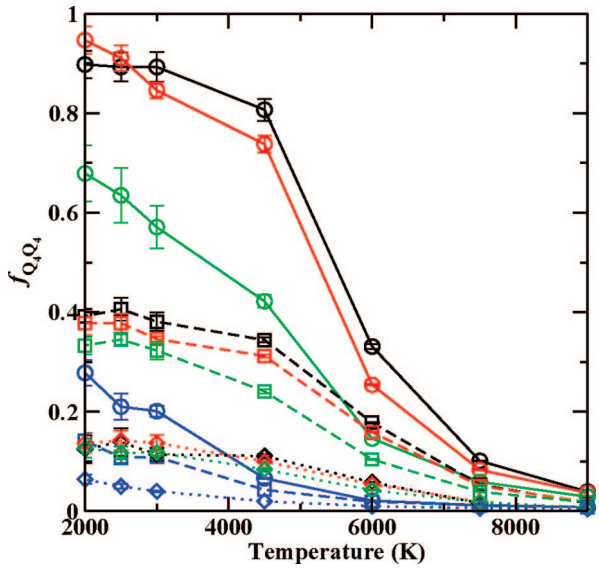

Figure 10. Fraction of Q_4 species corner-sharing with only Q_4 species as a function of temperature. Symbols and colors are the same as those in Figure 8.

In comparison, the coordination of Si around O atoms is not as dramatically affected by pressure. However, the composition dependence is much more pronounced for the oxygen coordination environment than for the silicon coordination environment (an observation that has also been made for hydrous $MgSiO_3$ melts).[24] This is to be expected because with increasing hydration a significant number of O−H bonds must be present. As was noted previously,[15] the value of f_{OSi_2} at 2000 K decreases linearly with composition at 1.0 GPa. For pure silica at $T \leq$ 6000 K, increasing the pressure leads to a marked increase in f_{OSi_3} and a concomitant decrease in f_{OSi_2}. At the highest temperatures ($T \geq$ 7500 K), the fraction of undercoordinated O atoms is greatly reduced at the higher pressures, and f_{OSi_2} at 10 GPa is slightly larger than at 0.25 GPa at 9000 K. For system 40W, an increase of the pressure to 10 GPa yields a decrease of f_{OSi_1} and an increase of f_{OSi_2} over the entire temperature range, whereas f_{OSi_3} remains insignificant for this highly hydrated melt.

An analysis of the Q_4 species can be used to examine intermediate and long-range tetrahedral structure. The notation Q_4 indicates that a Si atom has exactly 4 oxygen neighbors, each of which bridges to another Si atom, e.g. the second nearest neighbor of the central Si atom. Figure 9 shows the fraction of Q_4 species as a function of temperature for $x_w = 0.0$, 0.1, and 0.2. In general, f_{Q_4} decreases with temperature for a given composition and decreases with increasing x_w for a given temperature. With respect to pressure, f_{Q_4} is largest at the highest pressure while for the lower three pressures, the values are within 5% of each other for $p = 0.25$ to 2.5 GPa. The separation between f_{Q_4} at $p = 2.5$ and 10 GPa increases with increasing hydration and temperature.

The fraction of these Q_4 tetrahedra that corner-share with only other Q_4 tetrahedra is depicted in Figure 10. Here, the effects of pressure are most dramatic. For neat silica, when $p \leq 1.0$ GPa, $f_{Q_4Q_4}$ ranges from ≈90% at 2000 K to ≈4% at 9000 K. In contrast, for $p = 10$ GPa, $f_{Q_4Q_4} \approx 27\%$ at 2000 K and drops to less than 1% at 9000 K. Even at the intermediate pressure, 2.5 GPa, $f_{Q_4Q_4}$ is already significantly reduced over the entire temperature range compared to $p \leq 1.0$ GPa. The addition of 10 mol % water drops $f_{Q_4Q_4}$ to below 40% at 2000 K at all pressures and adding a further 10 mol % reduces $f_{Q_4Q_4}$ to less than 15%. For these hydrated melts, an increase in pressure from 0.25 to 2.5 GPa has a relatively modest effect on $f_{Q_4Q_4}$, but a further increase in pressure to 10 GPa reduces $f_{Q_4Q_4}$ by about a factor of 3 or more. For system 10W at $T = 2000$ K and $p =$ 1.0 GPa, an increase in the pressure to 10 GPa has a similar effect as an increase in the temperature to ≈ 6500 K.

3.4. Speciation. Table 2 summarizes the O coordination as a function of pressure for $x_w = 0.1$ at 3000 and 6000 K. The fractions of O atoms that are connected only to one or two H atoms (free hydroxide or molecular water, respectively) are less than 0.2% for all temperatures and pressures for system 10W. At 3000 K, the percentage of O atoms with exactly two Si neighbors remains constant near 90% up to 2.5 GPa and drops to 81% at 10 GPa. This decline is almost entirely balanced by a large increase in the percentage of O atoms with three Si neighbors which accounts for 13% of O atoms at 10 GPa but only 1.6% at 2.5 GPa. At the lower pressures, the remaining 10% of O atoms primarily have either one Si neighbor or one Si neighbor and one H neighbor (i.e., dangling hydroxyl groups). Overcoordinated O atoms account for less than 1% at $p \leq 1.0$ GPa, ≈2% at 2.5 GPa, and ≈15% at 10 GPa. This directly mirrors the trends in the CNs (see Figure 8). An increase in the temperature from 3000 to 6000 K leads to a decrease in the fraction of oxygen atoms bound to two atoms (bridging oxygens or dangling hydroxyl groups) and increases of the fraction of O atoms bound to one or three Si atoms.

The fraction of O atoms bound to exactly two H atoms (i.e., molecular water, $f_{H_2O_{mol}}$) and the natural logarithm of the equilibrium constant for silanol formation are given in Table 3 as a function of temperature and pressure for $x_w = 0.1$ and 0.4. Experimental evidence suggests that $f_{H_2O_{mol}}$ increases relative to f_{OH} as x_w increases in silicate glasses.[29] For $x_w = 0.1$, $f_{H_2O_{mol}}$ never accounts for more than 0.1% of O atoms. In contrast, for $x_w = 0.4$ at 2000 K, 2.1, 2.1, 1.7, and 1.4% of O atoms are present as molecular water at 0.25, 1.0, 2.5, and 10 GPa, respectively. At each pressure, the fraction of molecular water decreases with increasing temperature and with decreasing x_w.

TABLE 2: Percentage of O Atoms Found in Specific Neighbor Environments As a Function of Pressure for $x_w = 0.1$[a]

		3000 K				6000 K			
		p (GPa)							
total neighbors		0.25	1.0	2.5	10.0	0.25	1.0	2.5	10.0
1 neighbor	1 Si	5.4_2	5.3_2	4.3_2	2.4_2	8.3_2	7.6_1	6.6_1	3.8_1
2 neighbors	2 Si	89.9_2	89.9_3	90.2_1	81.2_6	83.7_2	83.2_1	80.0_2	68.9_2
	1Si,1H	4.2_2	3.9_2	3.2_1	1.5_1	2.1_1	1.9_3	1.8_1	1.3_1
3 neighbors	3 Si	0.1_1	0.5_2	1.6_6	12.8_5	5.0_1	6.3_1	10.2_2	22.6_2
	2Si,1H	0.2_1	0.3_1	0.6_1	1.7_1	0.7_1	0.9_1	1.1_1	2.0_1
>3 neighbors		0.0	0.0	0.0	0.3_1	0.1_1	0.1_1	0.3_1	1.4_1

[a] The values for one and two H neighbors are less than 0.2% and are not listed. The standard error of the mean is given as a subscript.

TABLE 3: Percentage of O Atoms Belonging to Molecular Water and Natural Logarithm of the Apparent Equilibrium Constant As Functions of Pressure and Temperature[a]

	0.25 GPa	1.0 GPa	2.5 GPa	10.0 GPa
		f_{H_2O}		
		$x_w = 0.1$		
2000 K	0.02_2	0.08_7	0.05_5	<0.01
2500 K	0.01_1	0.02_1	0.02_1	<0.01
3000 K	0.05_2	0.02_1	0.03_1	<0.01
4500 K	0.04_1	<0.01	<0.01	<0.01
6000 K	<0.01	<0.01	<0.01	<0.01
		$x_w = 0.4$		
2000 K	2.12_{14}	2.13_{20}	1.66_{11}	1.41_6
2500 K	1.84_{14}	1.35_{13}	1.22_2	1.30_5
3000 K	1.40_{13}	1.03_8	1.03_5	0.90_3
4500 K	0.95_8	0.73_2	0.61_1	0.57_1
6000 K	nal[b]	0.52_1	0.49_1	0.48_1
		ln K		
		$x_w = 0.1$		
2000 K	1.77_{26}	1.17_{42}	1.24_{33}	1.35_5
2500 K	1.77_9	1.58_{17}	1.45_{12}	1.34_8
3000 K	1.21_{24}	1.54_7	1.20_{10}	1.52_5
4500 K	1.57_4	1.54_6	1.60_3	1.79_2
6000 K	1.81_5	1.70_2	1.76_2	1.88_3
		$x_w = 0.4$		
2000 K	0.11_3	0.88_9	0.97_7	0.08_3
2500 K	0.56_2	1.37_8	1.32_2	0.38_3
3000 K	1.24_2	1.60_6	1.42_3	1.11_3
4500 K	1.48_5	1.71_2	1.76_1	1.61_1
6000 K	nal[b]	1.72_1	1.77_1	1.67_1

[a] A molecular water O atom is defined as an O atom with only two H neighbors, and $K = [OH_{melt}]^2/([O_{melt}][H_2O_{melt}])$ using the same species definitions as in ref 15. The standard error of the mean is given as a subscript. [b] Not a liquid.

This is in qualitative agreement with the experimental evidence.[29] Increasing the pressure leads to a reduction in $f_{H_2O_{mol}}$ for $T \leq 4500$ K. However, in particular for system 40W, the pressure effects on $f_{H_2O_{mol}}$ are relatively small compared to the changes in the liquid structure. In accord with the trends observed for $f_{H_2O_{mol}}$, it is found that ln K increases with increasing temperature and with decreasing x_w. For $x_w = 0.1$, the computed values of ln K for the FG silica melt fall within the range extrapolated from spectroscopic measurements (see Table 5 of ref 15 for rhyolitic and dacitic melts with total water concentrations of about 2.5 wt % at temperatures up to 1073 K).[30,31]

4. Conclusions

We have investigated structural and water speciation changes as a function of pressure and water mole fraction over a range of temperatures in the liquid SiO_2-H_2O system using Monte Carlo simulations for the empirical Feuston−Garofalini force field. The high-temperature volume minimum observed for neat silica and hydrated silica ($x_w = 0.1$)[15] vanishes at 10 GPa. Previous simulations have shown that the volume depression coincides with a change from a well-ordered tetrahedral SiO_2 network to a more disordered network.[15,27] At 10 GPa, this network is already significantly distorted, with O−O coordination numbers approaching the close packing limit.

Between 0.25 and 2.5 GPa, local and intermediate structures evolve gradually, as seen in the radial and angular distribution functions. This is true across all compositions. Greater changes in structure are seen at the highest pressure, including the rise in coordination noted above. Pressure effects are more apparent in longer range structure, as in $f_{Q_4Q_4}$, where the fraction of corner-sharing SiO_2 tetrahedra decreases by a factor of ≈1.3 from 0.25 to 2.5 GPa for pure silica at 2000 K and by another factor of ≈2.5 when the pressure is increased to 10 GPa.

The fraction of molecular water is largest for system 40W at 2000 K and $p \leq 1.0$ GPa ($f_{H_2O_{mol}} \approx 2.1\%$), and decreases with increasing temperature and pressure at constant x_w. Thus, under conditions similar to those in the Earth's mantle, molecular water is only present in very small proportion and the overwhelming fraction of water is dissociated and embedded in the silica network.

Acknowledgment. Financial support was provided by the National Science Foundation (ITR-0428774), the 3M Science and Technology and Louise Dosdall Fellowships (K.E.A.), and the Virtual Laboratory for Earth and Planetary Materials Summer Internship Program (L.C.G.). Computer resources were provided by the Minnesota Supercomputing Institute.

References and Notes

(1) Williams, Q.; Jeanloz, R. *Science* **1988**, *239*, 902.
(2) Xue, X.; Stebbins, J. F.; Kanzaki, M.; Tronnes, R. G. *Science* **1989**, *245*, 962.
(3) Meade, C.; Hemley, R. J.; Mao, H. K. *Phys. Rev. Lett.* **1992**, *69*, 1387.
(4) Tse, J. S.; Klug, D. D.; Le Page, Y. *Phys. Rev. B* **1992**, *46*, 5933.
(5) Somayazulu, M. S.; Sharma, S. M.; Garg, N.; Chaplot, S. L.; Sikka, S. K. *J. Phys.: Condens. Matter* **1993**, *5*, 6345.
(6) Sarnthein, J.; Pasquarello, A.; Car, R. *Phys. Rev. Lett.* **1995**, *74*, 4682.
(7) Della Valle, R. G.; Venuti, E. *Phys. Rev. B* **1996**, *54*, 3809.
(8) Roberts, M. M.; Wienhoff, J. R.; Grant, K.; Lacks, D. J. *J. Non-Cryst. Solids* **2001**, *281*, 205.
(9) Trave, A.; Tangney, P.; Scandolo, S.; Pasquarello, A.; Car, R. *Phys. Rev. Lett.* **2002**, *89*, 245504.
(10) Karki, B. B.; Bhattarai, D.; Stixrude, L. *Phys. Rev. B* **2007**, *76*, 104205.
(11) Hack, A. C.; Thompson, A. B.; Aerts, M. In *Reviews in Mineralogy and Geochemistry: Fluid-Fluid Interactions*; Liebscher, A., Heinrich, C. A., Eds.; Mineralogical Society of America: Washington, 2007; Vol. 65, pp 129−185, and references therein.
(12) Kennedy, G. C.; Wasserburg, G. J.; Heard, H. C.; Newton, R. C. *Am. J. Sci.* **1962**, *260*, 501.
(13) Holtz, F.; Roux, J.; Behrens, H.; Pichavant, M. *Am. Mineral.* **2000**, *85*, 682.
(14) Richet, P. *Phys. Chem. Glasses* **2005**, *46*, 333.
(15) Anderson, K. E.; Hirschmann, M. M.; Siepmann, J. I. *J. Phys. Chem. B* **2008**, *112*, 13005.
(16) McDonald, I. R. *Mol. Phys.* **1972**, *23*, 41.
(17) Feuston, B. P.; Garofalini, S. H. *J. Phys. Chem.* **1990**, *94*, 5351.
(18) Litton, D. A.; Garofalini, S. H. *J. Appl. Phys.* **2001**, *89*, 6013.
(19) Hudon, P.; Jung, I.-H.; Baker, D. H. *Phys. Earth Planet. Interior* **2002**, *130*, 159.
(20) Kuzuu, N.; Yoshie, H.; Tamai, Y.; Wang, C. *J. Non-Cryst. Solids* **2004**, *349*, 319.
(21) Pitzer, K. M.; Sterner, S. M. *J. Chem. Phys.* **1994**, *101*, 3111.
(22) Matsukage, K. N.; Jing, Z. C.; Karato, S. *Nature* **2005**, *438*, 488.
(23) Sakamaki, T.; Suzuki, A.; Ohtani, E. *Nature* **2006**, *439*, 192.
(24) Mookherjee, M.; Stixrude, L.; Karki, B. *Nature* **2008**, *452*, 983.
(25) Angell, C. A.; Cheeseman, P. A.; Tamaddon, S. *Science* **1982**, *218*, 885.
(26) Stixrude, L. In *Structure and Imperfections in Amorphous and Crystalline Silicon Dioxide*; Devine, R. A. B., Duraud, J.-P., Dooryhée, E., Eds.; Wiley: Chichester, England, 2000; pp 69−103.
(27) Perchak, D. R.; O'Reilly, J. M. *J. Non-Cryst. Solids* **1994**, *167*, 211.
(28) Hemley, R. J.; Prewitt, C. T.; Kingma, K. T. In *Reviews in Mineralogy: Silica: Physical Behavior, Geochemistry, and Materials Applications*; Heaney, P. J., Prewitt, C. T., Gibbs, G. V., Eds.; Mineralogical Society of America: Washington, 1994; Vol. 29, pp 41−81.
(29) Kohn, S. C. *Mineral. Mag.* **2000**, *64*, 389.
(30) Novak, M.; Behrens, H. *Earth Planet. Sci. Lett.* **2001**, *184*, 515.
(31) Liu, Y.; Behrens, H.; Zhang, Y. X. *Am. Mineral.* **2004**, *89*, 277.

JP802255Y